

Aquatic Habitat Bottom Classification Using ADCP

F. Douglas Shields Jr., M.ASCE¹

Abstract: Description of physical aquatic habitat often includes data describing distributions of water depth, velocity, and bed material type. Water depth and velocity in streams deeper than about 1 m may be continuously mapped using an acoustic Doppler current profiler from a moving boat. Herein we examine the potential of using the echo signal strength from the bed as an indicator of bed material type. Mean signal strength from soft muddy beds was consistently 10–20 dB lower than mean signal strength from noncohesive (gravel or sand) beds. Sand beds tended to have larger site-to-site variation (means –30 to –19 dB) than for fines (–43 to –38 dB) or gravel (–23 to –20 dB).

DOI: 10.1061/(ASCE)HY.1943-7900.0000181

CE Database subject headings: Sediment; Acoustic techniques; Aquatic habitats; River beds.

Author keywords: River; Bottom classification; Physical habitat; Sediment; Acoustics; Doppler.

Introduction

Restoration or rehabilitation of degraded aquatic habitats requires definition of a target condition and preferably postimplementation monitoring to measure progress toward the target. A physical habitat condition, rather than some state of biotic populations, is often selected as a target because biotic conditions are more difficult to sample and describe and often exhibit great variation driven by variables outside the stream ecosystem (e.g., climate or ocean events). Physical lotic habitat has been described as the joint distribution of water depth, water velocity, bed type, and sometimes cover (e.g., Gorman and Karr 1978 and Shields et al. 1994). Practically, stream habitat has been characterized by computing statistics based on measurements of water depth and velocity at each point of a horizontal grid. In many cases stream bed type and cover, both qualitatively assessed, were included as additional grid variables. Resultant statistics describing the central tendency, variability, and spatial distribution of these three or four variables, and their combinations have been used to explain key differences between more- and less-degraded streams and to infer biotic responses. Usually the required data are collected by wading observers.

Collection of water depth and velocity information may be automated across a wide range of stream sizes using an acoustic Doppler current profiler (ADCP). These data have also been used to study water column (Shields and Rigby 2005) and benthic (Gaeuman and Jacobson 2007) habitats in streams. Here we suggest that ADCP data may also be used to infer bed hardness and thus bed sediment type. Many workers have proposed methods for using specialized equipment and software to acoustically explore or classify underwater sediments (Chivers et al. 1990;

Mac Dougall and Black 1999; Hamilton et al. 1999) and submersed aquatic vegetation (Hoffman et al. 2002). These systems have been primarily applied to marine environments with mixed success, but some work has been reported in lakes and rivers (Edsall et al. 1997; Preston et al. 2000; Cholwek et al. 2000, 2005), and research and development are ongoing (Wienberg and Bartholomä 2005; Anderson et al. 2008; McGonigle et al. 2009). Commercially available bottom classification systems generally cost between \$15,000 and \$40,000, including software and hardware. Here we propose using ADCPs, which are already in wide use for discharge measurements, to map the distribution of surficial bed sediment type while simultaneously mapping water depth and current profiles. Bottom types may be determined by extracting the return signal strength from the bottom track echo and using this information to compute the echo intensity (EI) at the bed. Bed EI is a function of the sediment bulk density, the amount of gas in voids near the bed surface, and the geometric uniformity (flatness) of the bed. All of these qualities are related directly or indirectly to sediment grain size and transport regime, although “there is no simple relationship between the backscatter signal and surficial sediment type and structure” (Anderson et al. 2008). The discussion below is based on use of a Teledyne RDI 1200 kHz Workhorse Rio Grande ADCP in streams, rivers, and lakes with depths ranging from 1 to 7 m and velocities ranging from 0 to 2.5 m·s⁻¹.

Computations

The EI detected by the instrument is given by (Gordon 1996)

$$EI = SL + SV + K - 20 \log(R) - 2\alpha R \quad (1)$$

where EI=echo intensity recorded by the instrument (dB); SL=source level or transmitted power 1 m from transducer (dB); SV=bottom backscattering strength (dB); K=transducer-specific constant based on the relationship between pressure at the transducer face and the measured signal strength; R=distance from the transducer to the bottom measured along the beam (m)= $r/\cos \theta$, where r is the vertical distance from the transducer to the bottom (m) and θ is the beam angle (20°); and α =sound absorption coefficient (dB/m).

¹Research Hydraulic Engineer, National Sedimentation Laboratory, USDA Agricultural Research Service, P.O. Box 1157, Oxford, MS 38655-1157. E-mail: doug.shields@ars.usda.gov

Note. This manuscript was submitted on March 16, 2009; approved on October 24, 2009; published online on November 9, 2009. Discussion period open until October 1, 2010; separate discussions must be submitted for individual papers. This technical note is part of the *Journal of Hydraulic Engineering*, Vol. 136, No. 5, May 1, 2010. ©ASCE, ISSN 0733-9429/2010/5-336–342/\$25.00.

Table 1. General Characteristics of Reaches Sampled for Bottom Signal Strength

Water body	Environment	Bed type	Water depth (m)	Mean current velocity (m·s ⁻¹)
Big Sunflower River	Channelized river	Silt and clay	1–5	0.02–0.03
Holly Bluff Cutoff Channel	Straight manmade flood control channel	Sand and clay	7.8	0.2
Deep Hollow Lake	Natural oxbow	Silt and clay	1.0	—
Little Tallahatchie River	Meandering river	Sand and gravel	1–4	0.3–0.7
Luxapalila Creek	Channelized river	Fine gravel and sand	1–4	0.06–0.14
Sylamore Creek	Meandering river	Gravel	2.9	0.02
White River	Meandering river	Sand	2.6	1.1
		Gravel	2.5–2.8	0.6–0.7

The last two terms account for signal strength decay due to beam spreading and absorption of acoustic energy, respectively. Solving for $SV+K$, which we denote dB^*

$$dB^* = SV + K = EI - SL + 20 \log(R) + 2\alpha R \quad (2)$$

Below we compute dB^* for various river and lake bottom types and compare results. The EI was determined by converting the return signal strength indicator (RSSI) recorded by the ADCP in “counts” to units of dB by multiplying RSSI by the EI scale factor using an empirical formula (no rational units) supplied by the manufacturer

$$\text{scale factor} = \frac{127.3}{(273 + T_e)} \quad (3)$$

where T_e =temperature of the instrument in °C, assumed equal to the water temperature.

SL is given by the equation

$$SL = 10 \log\left(\frac{P}{P_0}\right) \quad (4)$$

where P_0 =reference pressure (1 μPa) and P =pressure of the signal propagated by the ADCP, given by

$$P = \sqrt{\rho c I} \quad (5)$$

where ρ =density of the medium (kg m⁻³); c =speed of sound (assumed to be constant=1,450 m·s⁻¹); and I =power density (W m⁻²).

Power density, I , was computed by assuming the transmitted power is spread out over a surface area equal to the area of a circle with a diameter equal to one beamwidth at a distance of 1 m from the transducer

$$I = \frac{4A_{\text{rms}}V_{\text{rms}}P_F E}{\pi d^2} \quad (6)$$

where A_{rms} =root-mean-square (rms) current for transmitted signal (amp); V_{rms} =rms voltage for transmitted signal (volts); P_F =power factor (assumed=0.5); E =efficiency (assumed=0.5); and d =beam diameter (m) at a distance of 1 m from transducer, assumed equal to transducer diameter, 0.054 m (personal communication, Kent Deines).

The transmit voltage and current were obtained from the binary output file (RD Instruments 2001, p. 122) and converted from counts to amps and volts as follows:

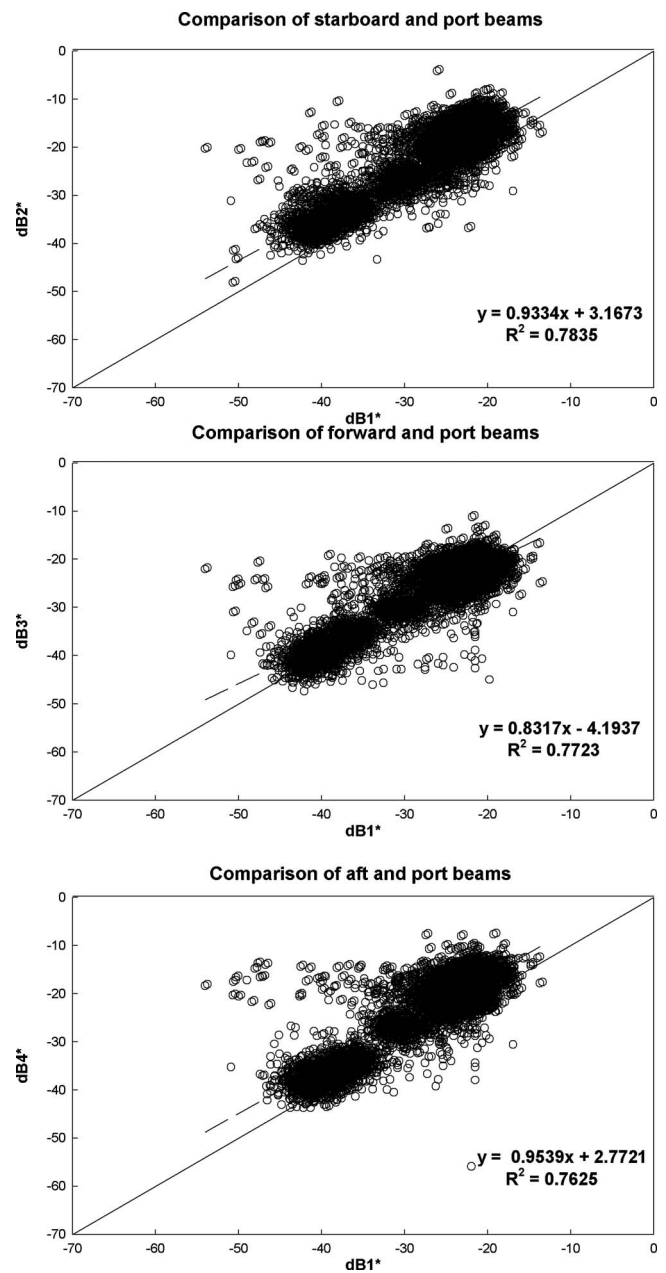


Fig. 1. Comparison of simultaneous measurements of bottom back-scattering strength using different transducers on the same ADCP

Table 2. Mean Bottom Backscattering Strength, dB^* , for Low-Energy Sites

Water body	Bed type	% by weight				Number of values	Mean dB^*	Std. dev.
		Gravel	Sand	Silt	Clay			
Big Sunflower River	Silty clay	0	3	40	56	319	-38	1.5
		0	17	45	38	263	-40	1.2
		0	8	38	55	435	-42	1.0
		0	14	44	42	507	-38	1.0
Deep Hollow Lake	Silt	$D_{50}=0.012$ mm, mean= 0.043 mm, std. dev.= 0.063 mm ^a				388	-43	1.3
Little Tallahatchie River	Silty sand	0	77	23 ^b		71	-31	1.2
Big Sunflower River	Sand	0	100	0	0	189	-24	3.4
Holly Bluff Cutoff Channel	Silty, clayey sand	0	70	10	20	433	-32	0.9
Luxapalila Creek	Sand	8	91	1	0	138	-30	3.5
		4	96	1	0	152	-23	1.3
		86	14	0	0	151	-22	1.0
Oil Creek	Sandy gravel	73	27	0	0	207	-23	1.3
Sylamore Creek	Gravel	96	4	0	0	1,524	-23	1.2

^aStatistics are for five bed samples collected at three locations along the lake centerline.

^bSilt+clay.

$$A_{\text{rms}} = 0.011451 \times \text{ADC counts}$$

$$V_{\text{rms}} = 0.253765 \times \text{ADC counts}$$

Transducer constants, K , were unknown, but it was assumed that each of the four transducers on a given ADCP would have different constant values. We adjusted dB^* values from transducers 2–4 to a common reference based on regression against dB^* values measured simultaneously by transducer 1.

Because the sound beam is approximately cylindrical in the near field and then spreads as a cone in the far field, the expression for beam spreading, $20 \log(R)$, is valid only for R in excess of a near-zone distance. The near-zone distance is specified by the ADCP manufacturer as $R=2.1$ m (RD Instruments 2003). For computation, the value of R in the term $20 \log(R)$ was replaced by the value computed using the following empirical expression (Libicki et al. 1989 in Thorne et al. 1991) whenever $0.4 < R \leq 2.1$ m. Values with $R < 0.4$ m were discarded

$$R \times \left[\frac{2 + \frac{\epsilon r_n}{R}}{3} \right] \quad (7)$$

where $\epsilon=1$ and $r_n=2.1$ m.

The sound absorption coefficient, α , is dependent on water temperature, salinity, and suspended sediment particle size and concentration (Liu and Li 2008; Elci et al. 2008). For example, Liu and Li (2008) showed that the value of α for a 25 kHz signal doubled as the concentration of fine sediment in water increased from 0.15 to 0.75% by weight. However, we used a 1200 kHz system in water with suspended sediment concentrations that were at least two orders of magnitude lower than these. Variation over the range of water temperatures observed in this study is slight, and no information was available regarding suspended sediment concentrations at our study sites. Visual observations and comparison of depth-averaged velocity values to bed sediment size indicated that sediment concentrations were very low (~ 10 – 100 mg/L). Therefore a constant value of 0.35 dB m^{-1} was assumed based on the work of Francois and Garrison (1982a,b) and National Physical Laboratory (2009) for α given an assumed temperature of 19°C , 1228.28 kHz frequency in freshwater. This assumption likely introduced some error at the higher-

energy sand bed sites since a moving bed layer or sediment suspended in the water column would increase sound absorption. This possibility was examined by analyzing the relationship between dB^* and depth-averaged velocity for sand bed sites with velocities of >0.2 $m \cdot s^{-1}$.

Data Collection

Bottom track data were collected using a 1,228.28 kHz Teledyne RDI Rio Grande Workhorse ADCP from an aluminum boat anchored in a range of fluvial environments as shown in Table 1. With the exception of Deep Hollow Lake, where data were composited from several anchoring points, each anchoring point is referred to below as a “site.” Sites were selected to represent a range of bed types, and samples of bed material were collected at each site with either a BM60 bed material sampler or a petite Ponar dredge. Qualitative visual descriptions were recorded for each bed sample, and sediments were returned to the lab and subjected to standard analysis for grain size distributions. Additional ADCP data were collected from river reaches encompassing the points where bed samples had been collected.

Analysis

Values for dB^* were computed using the procedure outlined above. Initial analysis focused on ensembles with good data for all four beams. Beams 1 and 3 (which point port and forward, respectively) produced dB^* site means within 1–5% of each other while Beams 2 and 4 (pointing starboard and aft, respectively) produced site means within 2–22% of each other. The four beams ensonify regions of the bed that are separated by a distance that is roughly 70% of the water depth. Although some scatter in beam signatures is therefore due to local differences in bed conditions, we assumed that, on average, regions simultaneously ensonified by the four beams were similar and that differences in beam signatures were due to transducer-specific characteristics. Therefore Beams 2–4 were corrected to the same relative magnitude as Beam 1 using regression formulas based on data ensembles with good values for all four beams (Fig. 1). The scatter in the rela-

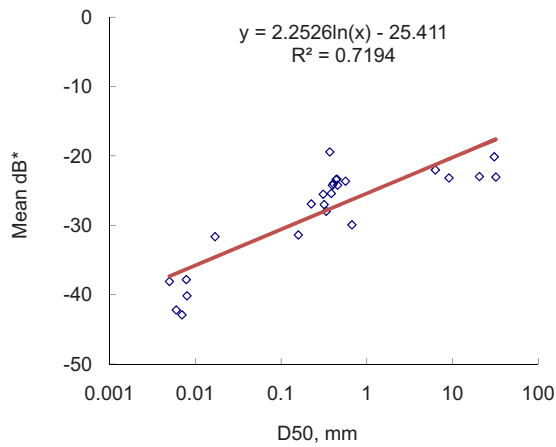


Fig. 2. Mean dB^* for river and lake sites versus median bottom sediment size. Each point represents the average dB^* for a given fixed point except for point for Deep Hollow Lake (0.012 mm, -43 dB), which represents composite of five bed samples collected at three locations along the lake centerline.

tionships shown in Fig. 1 is likely at least partially due to differences in bed conditions encountered by the beams. After correction, correlation coefficients and coefficients of determination were computed between dB^* and each term in Eq. (1). Mean dB^* values were computed for the four beams in each ensemble, and frequency distributions were computed for each site and for each major sediment type and hydraulic environment.

When sites with a wide range of sediment sizes were considered, site-to-site variation in dB^* appeared highly correlated with median bed sediment grain size. However, site-to-site variation for sand bed sites with mean current velocities $>0.2 \text{ m}\cdot\text{s}^{-1}$ was greater than for other bed types, perhaps because of variation in bed forms or the presence of an active bed load layer. Accordingly, multiple linear regression was used to examine the relationship between dB^* , D_{50} , and depth-averaged velocity for these sites. Depth-averaged velocities were computed for fixed point data using time-averaged velocity profiles obtained with the ADCP.

Table 3. Mean Bottom Backscattering Strength, dB^* , for High-Energy Sites

Water body	Bed type	% by weight			No. of values	Mean dB^*	Std. dev.
		Gravel	Sand	Fines			
Little Tallahatchie River	Sand	0	98	1	210	-27	1.4
		0	100	0	95	-24	1.3
		1	99	0	44	-23	0.7
		0	100	0	39	-26	0.9
		1	99	0	57	-24	0.9
		0	100	0	61	-27	0.8
White River	Sand and hard clay	3	90	7	61	-28	1.5
		15	80	5	170	-25	1.0
	Gravelly sand	28	72	0	208	-24	1.2
		0	89	11	164	-19	1.0
Gravel	99	1	0	344	-20	1.2	
	93	6	1	345	-23	3.2	

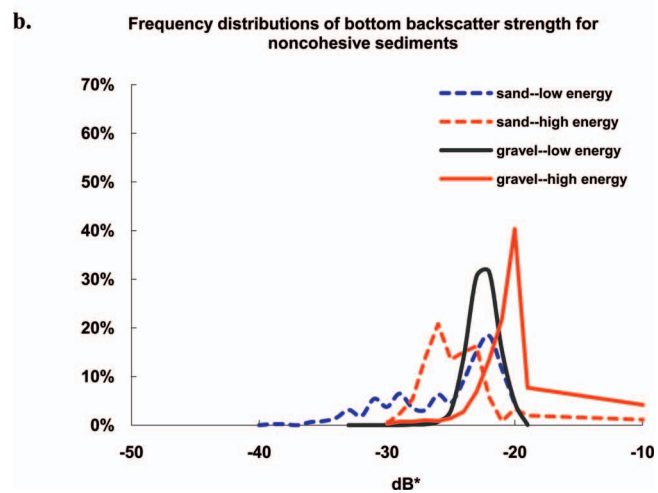
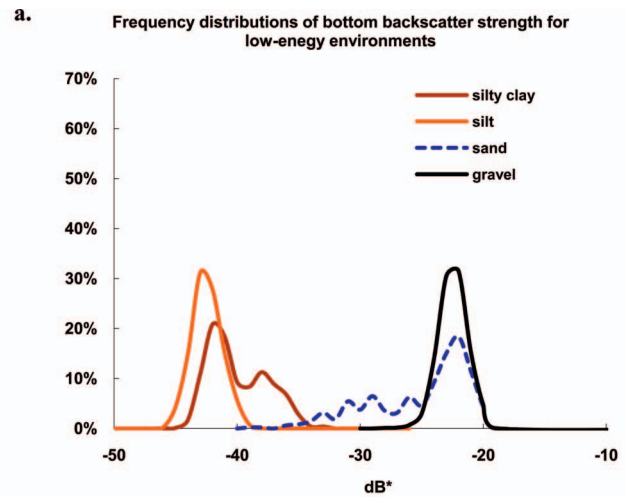


Fig. 3. (Color) Frequency distributions for dB^* measured over various types of river bed sediments: (a) low-energy environments; (b) sands and gravels in low- and high-energy environments. Distributions are smooth curves drawn through frequency histograms with 1 dB bin interval.

An entire meander bend of the Little Tallahatchie River in Mississippi was acoustically scanned on the same day that point samples of sediment and bottom backscatter strength were obtained. Resulting data were used to generate contour maps of bottom backscatter strength, water depth, and current velocity in order to create a synoptic view of physical aquatic habitat.

Results

Between 39 and 1,524 measured dB^* values and bed sediment samples were collected from 24 fixed points (sites) representing a wide range of aquatic environments. An additional 388 dB^* values and five bed sediment samples were collected from fixed points distributed along the centerline of a homogeneous shallow oxbow lake; these were combined to represent a single “site” by averaging the median grain sizes (Table 2). From 63% to 85% of the variation in dB^* was due to variation in EI, the bottom EI, for a database comprised of 6,575 measurements. Power level varied little within our data set, and r^2 values between dB^* values for

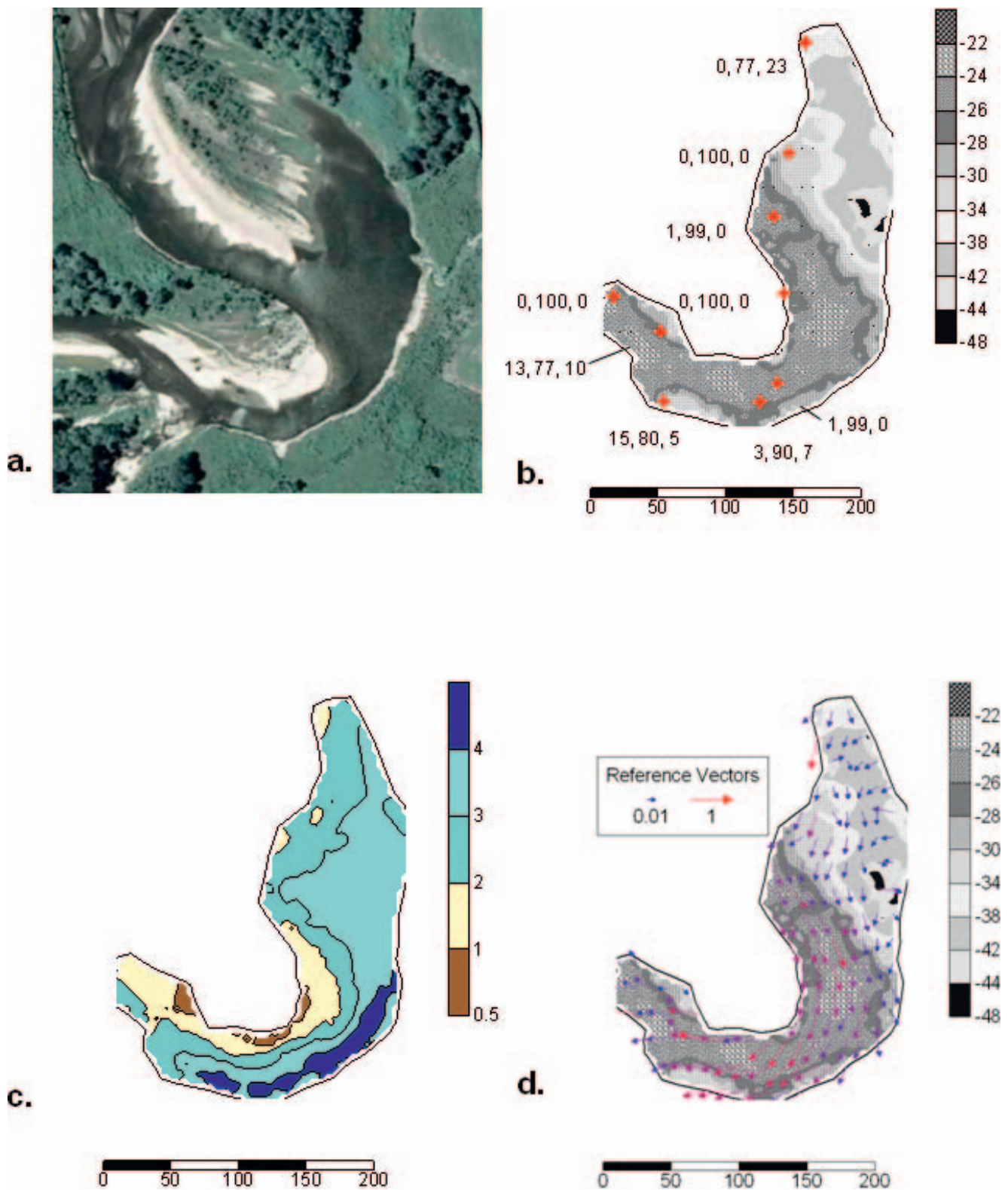


Fig. 4. (Color) Habitat maps for Jones Creek bend, Little Tallahatchie River, Mississippi based on ADCP data collected September 11, 2008. (a) Air photograph taken August 11, 2007 with water level about 1.6 m lower than for ADCP collection one year later. However, note tributary mouth at lower left of photo and backwater area at upper right. (b) Average bottom return signal strength dB^* in dB. Red crosses show points where bed samples and simultaneous 5 min stationary boat ADCP runs were collected. Numbers represent percent gravel, sand, and fines for bed samples. (c) Water depth in m. (d) Average bottom return signal strength shown in panel (b) with depth-averaged water velocity vectors ($m \cdot s^{-1}$) superimposed.

each beam and SL ranged from 2 to 3%. The variation in terms in Eq. (2) representing losses due to beam spreading and sound absorption in the water column accounted for 4% to 8% and 8% to 13% of the variation in dB^* , respectively. The adequacy of Eq. (2) to correct the return signal strength for depth effects was examined by correlating dB^* with water depth. Water depth explained less than 15% of the variation in dB^* across our entire data set. This correlation appeared to be the result of the fact that water depths from sites with fine-grained sediments ranged up to 8.3 m while depths from sites with sand or gravel beds were limited to 4.3 m or less.

For all sampled sites, median bottom sediment grain size explained about 72% of the variance in site-mean dB^* (Fig. 2). A nonparametric analysis of variance (Kruskal-Wallis with Dunn's method for pairwise comparisons) using the bed types for each site (Tables 2 and 3) indicated significant differences in dB^* distributions ($p < 0.05$) among all of the assigned classifications that were not mixtures of one or more types. For example, gravel and sand were significantly different, but sand and gravelly sand were not.

Closer exploration of data focused on well-sorted (narrowly graded) sediments from quiescent environments (lakes or low-velocity rivers). Frequency distributions associated with each major sediment type (sites pooled) are provided in Fig. 3(a) and summary statistics for each fixed point (site) are shown in Table 2. Cohesive and noncohesive bed material had distinct signatures. Gravel beds produced backscatter strengths about 10–20 dB greater than for soft muddy bottoms. Sandy bottoms had backscatter strengths intermediate to mud and gravel, and sand produced a much wider range of dB^* than other bed types [Fig. 3(a)].

Examination of data from similar well-sorted beds located in higher-energy environments indicated that sands and gravels produce similar average backscatter strengths, but that sand again had much higher variance [Fig. 3(b)], perhaps due to sand transport or bed forms. Apparently the greater variation among sandy sites reflects the more dynamic structure of sandy beds. Bed forms, saltating particles, and suspended particles all influence acoustic signatures (Thorne and Hanes 2002). In general however, standard deviations of dB^* for single sand sites were not likely to be larger than standard deviations from single gravel sites (Tables 2 and 3).

The higher mean dB^* of -19 dB for sand from the White River sand site relative to the Little Tallahatchie sites (-27 to -23 dB) (Table 3) may be related to bed roughness. Bathymetric data from the ADCP indicated that the White River sand site had a plane bed while the Little Tallahatchie sites (Table 3) exhibited dunes. About 84% of the variation in mean dB^* from fixed points over sand beds with mean current velocity >0.2 m·s $^{-1}$ was explained by a regression formula based on grain size- and depth-averaged velocity, with higher values of dB^* from coarser beds with higher velocity. Median bed material size alone explained 22% of variation in dB^* , while velocity alone explained 60%. The velocity correlation was largely due to the presence of the aforementioned White River site, which had a sandy plane bed. Median bed sediment size for all 10 of the high-energy sand bed sites ranged from 0.23 to 0.56 mm, and D_{84} values were between 0.4 and 11.9 mm.

Contour maps of dB^* , water depth, and current velocity for a large complex bend of the Little Tallahatchie River are presented in Fig. 4. "Ground truth" for the dB^* measurements was obtained by sampling bed sediments and bottom backscatter strength simultaneously as described above at the points shown

as red crosses in Fig. 4(b). The three numbers adjacent to the crosses indicate the composition of bed samples as gravel, sand, and fines in percent by weight. Bottom habitats were complex, exhibiting the influence of bend flow hydraulics and inflows of coarse sediments from a tributary mouth on the downstream left descending bank. A large area of finer sediments on the upstream left descending bank was associated with a slackwater overflow channel.

Conclusion

Synoptic maps of three of the major components of riverine physical aquatic habitat, current velocity, water depth, and bottom type can be made using commercially available boat-mounted ADCP. However, conversion of signal strength values recorded by the instrument to bottom hardness requires use of instrument-specific coefficients that must be obtained by ground truthing each ADCP using bed sediment samples and ADCP data collected simultaneously. Furthermore, the return signal strength for sandy bottoms apparently varies widely based on bed forms and sediment bulk density. Soft bottom (mud, clay, and silt) can be distinguished from noncohesive sediment bottoms, but sand beds could not reliably be discriminated from gravel.

Application

Workers interested four-beam acoustic Doppler profiler data to study aquatic habitats might proceed as follows:

1. Develop relationships among the four-beam responses similar to those shown in Fig. 1 using data collected over a variety of sediment types. Ideally, each site should have relatively homogeneous sediment and topographic conditions;
2. Using the Doppler coupled with high-resolution global positioning system and perhaps an echo sounder, collect data while anchored at selected fixed points that are representative of the hydraulics and sediment types found in the reach of interest [e.g., Fig. 4(b)]. A minimum sampling time of five minutes at each fixed point is recommended. Collect synoptic bed sediment samples from the same points and obtain size distributions using standard approaches;
3. Post-process the resulting data to obtain dB^* values using Eq. (1);
4. Examine data from fixed points to related dB^* signatures to sediment size, density, and transport regime; and
5. Generate maps or other summaries of physical habitat quality.

Acknowledgments

Kent Deines and Doug Shields Sr. provided helpful suggestions and insights. Sam Testa and John Massey assisted with field data collection. Daniel Wren, Colin Rennie, Roger Kuhlne, and David Mueller read an earlier version of this paper and made many helpful suggestions.

References

- Anderson, J. T., Holliday, D. V., Kloser, R., Reid, D. G., and Simard, Y. (2008). "Acoustic seabed classification: Current practice and future

- directions." *ICES J. Mar. Sci.*, 65, 1004–1011.
- Chivers, R. C., Emerson, N., and Burns, D. R. (1990). "New acoustic processing for underway surveying." *Hydrographic J.*, 56, 9–17.
- Cholwek, G., Bonde, J., Li, X., Richards, C., and Yin, K. (2000). "Processing RoxAnn sonar data to improve its categorization of lake bed surficial substrates." *Mar. Geophys. Res.*, 21, 409–421.
- Cholwek, G., Yule, D., Eitrem, M., Quinlan, H., and Doolittle, T. (2005). *Mapping potential lake sturgeon habitat in the lower Bad River complex*, U.S. Geological Survey Great Lakes Science Center, Ann Arbor, Mich.
- Edsall, T. A., Behrendt, T. E., Cholwek, G., Frey, J. W., Kennedy, G. W., and Smith, S. B. (1997). *Use of remote-sensing techniques to survey the physical habitat of large rivers*, U.S. Geological Survey Great Lakes Science Center, Ann Arbor, Mich.
- Elci, S., Aydin, R., and Work, P. A. (2008). "Estimation of suspended sediment concentration in rivers using acoustic methods." *Environ. Monit. Assess.*, 159(1–4), 1573–2959.
- Francois, R. E., and Garrison, G. R. (1982a). "Sound absorption based on ocean measurements. Part I: Pure water and magnesium sulfate contributions." *J. Acoust. Soc. Am.*, 72(3), 896–907.
- Francois, R. E., and Garrison, G. R. (1982b). "Sound absorption based on ocean measurements. Part II: Boric acid contribution and equation for total absorption." *J. Acoust. Soc. Am.*, 72(6), 1879–1890.
- Gaeuman, D., and Jacobson, R. B. (2007). "Quantifying fluid and bed dynamics for characterizing benthic physical habitat in large rivers." *J. Appl. Ichthyol.*, 23, 359–364.
- Gordon, R. L. (1996). *Acoustic Doppler current profiler: Principles of operation, a practical primer*, RD Instruments, San Diego.
- Gorman, O. T., and Karr, J. R. (1978). "Habitat structure and stream fish communities." *Ecology*, 59(3), 507–515.
- Hamilton, L. J., Mulhearn, P. J., and Poeckert, R. (1999). "Comparison of RoxAnn and QTC-View acoustic bottom classification system performance for the Cairns area, Great Barrier Reef, Australia—Regional variation in a terrigenous-carbonate province." *Cont. Shelf Res.*, 19(12), 1577–1597.
- Hoffman, J. C., Burczynski, J., Sabol, B., and Heilman, M. (2002). "Digital acoustic system for ecosystem monitoring and mapping: assessment of fish, plankton, submersed aquatic vegetation, and bottom substrata classification." *Proc., 2001 Conf. of Fisheries and Aquatic Sciences Working Group*, International Council for the Exploration of the Sea, Seattle.
- Libicki, C., Bedford, K. W., and Lynch, J. F. (1989). "The interpretation and evaluation of a 3MHz acoustic backscatter device for measuring benthic boundary layer sediment dynamics." *J. Acoust. Soc. Am.*, 85, 1501–1511.
- Liu, Y., and Li, Q. (2008). "Research on the coefficient of sound absorption in turbid water." *J. Marine Science Applications*, 7, 135–138.
- Mac Dougall, N., and Black, K. D. (1999). "Determining sediment properties around a marine cage farm using acoustic ground discrimination: RoxAnn." *Aquacult. Res.*, 30, 451–458.
- McGonigle, C., Brown, C., Quinn, R., and Grabowski, J. (2009). "Evaluation of image-based multibeam sonar backscatter classification for benthic habitat discrimination and mapping at Stanton Banks, UK." *Estuarine Coastal Shelf Sci.*, 81, 423–437.
- National Physical Laboratory. (2009). "Calculation of absorption of sound in seawater." (<http://resource.npl.co.uk/acoustics/techguides/seaabsorption/>) (March 5, 2009).
- Preston, J. M., Rosenberger, A., and Collins, W. T. (2000). "Bottom classification in very shallow water." *Oceans 2000 MTS/IEEE Conf. and Exhibition*, Quester Tangent Corp., Sidney, Canada, 1563–1567.
- RD Instruments. (2001). "Workhorse commands and output data format." *P/N 957-6156-00*, RD Instruments, San Diego.
- RD Instruments. (2003). *WinRiver Application 1.06. Help screens*, RD Instruments, San Diego.
- Shields, F. D., Jr., Knight, S. S., and Cooper, C. M. (1994). "Effects of channel incision on base flow stream habitats and fishes." *Environ. Manage. (N.Y.)*, 18(1), 43–57.
- Shields, F. D., Jr., and Rigby, J. R. (2005). "River habitat quality from river velocities measured using acoustic Doppler current profiler." *Environ. Manage. (N.Y.)*, 36(4), 565–575.
- Thorne, P. D., and Hanes, D. M. (2002). "A review of acoustic measurement of small-scale sediment processes." *Cont. Shelf Res.*, 22, 603–632.
- Thorne, P. D., Vincent, C. E., Hardcastle, P. J., Rehman, S., and Pearson, N. (1991). "Measuring suspended sediment concentrations using acoustic backscatter devices." *Mar. Geol.*, 98, 7–16.
- Wienberg, C., and Bartholomä, A. (2005). "Acoustic seabed classification in a coastal environment (outer Weser Estuary, German Bight)—A new approach to monitor dredging and dredge spoil disposal." *Cont. Shelf Res.*, 25, 1143–1156.